

## Carmichaelite, a new hydroxyl-bearing titanate from Garnet Ridge, Arizona

LIPING WANG,\* ROLAND C. ROUSE, ERIC J. ESSENE, DONALD R. PEACOR, AND YOUXUE ZHANG

Department of Geological Sciences, University of Michigan, Ann Arbor, Michigan 48109-1063, U.S.A.

### ABSTRACT

Carmichaelite  $[\text{MO}_{2-x}(\text{OH})_x]$ , where M includes Ti, Cr, Fe, Mg, and Al) is a new hydrous titanate from Garnet Ridge, an ultramafic diatreme on the Colorado Plateau in Arizona. It is named in honor of Ian S.E. Carmichael, Professor of Geology at the University of California, Berkeley, in recognition of his many contributions to petrology, especially his studies of Fe-Ti oxides in volcanic rocks. The new mineral occurs as platy, cinnamon-brown inclusions in mantle-derived pyrope crystals, which also contain inclusions of rutile, srilankite, ilmenite, minerals of the crichtonite group, spinel, and olivine. Carmichaelite is commonly in contact with rutile and occasionally with srilankite. The average composition is  $\text{TiO}_2 = 62.16$ ,  $\text{Cr}_2\text{O}_3 = 18.43$ ,  $\text{Al}_2\text{O}_3 = 1.88$ ,  $\text{V}_2\text{O}_5 = 0.87$ ,  $\text{Nb}_2\text{O}_5 = 0.37$ ,  $\text{FeO} = 7.61$ ,  $\text{MgO} = 2.80$ ,  $\text{H}_2\text{O (calc)} = 5.76$ , total 99.89 wt%, giving an empirical formula close to  $\text{Ti}_{0.62}\text{Cr}_{0.19}\text{Fe}_{0.09}\text{Mg}_{0.06}\text{Al}_{0.03}\text{V}_{0.01}\text{O}_{1.5}(\text{OH})_{0.5}$ . A cation (non-H) to (O+OH) ratio of 1:2 was confirmed by microprobe analysis of oxygen, and the presence of the hydroxyl component was supported by IR data. Carmichaelite is monoclinic, space group  $P2_1/c$ , with  $a = 7.706(1)$ ,  $b = 4.5583(6)$ ,  $c = 20.187(3)$  Å,  $\beta = 92.334(2)^\circ$ ,  $V = 708.5(3)$  Å<sup>3</sup>, and  $Z = 22$ . The calculated density is 4.13 g/cm<sup>3</sup>. The strongest diffraction lines [ $d(I, h k l)$ ] from a calculated powder pattern are 2.842 (100,  $\bar{1}15$ ), 3.773 (94, 013), 2.664 (70, 213), 1.688 (54,  $\bar{3}22$ ), 1.679 (44, 226), 1.661 (44,  $\bar{1}28$ ), and 1.648 (34, 1.1.11). The crystal structure, which has been determined from single-crystal X-ray diffraction data, consists of stacked chains of cation octahedra within layers of hexagonal closest-packed anions. The arrangement of cation octahedra within a single chain has the same basic structural unit of five edge-sharing octahedra found in olivine, the humite group, and leucophoenicite.

Carmichaelite is inferred to have co-precipitated with its pyrope host and other titanates in the presence of a fluid or melt phase (i.e., mantle metasomatism) at temperatures of 650–750 °C and pressures of 20–25 kbar. It contains the highest OH content reported for titanates of mantle origin and offers a potential storage site for water and high field strength elements in the upper mantle. The new mineral is probably stabilized by high pressure and the high concentration of Cr. Certain features of the carmichaelite structure raise the possibility of a similar high-pressure phase in the Si-Al-O-H system.

### INTRODUCTION

Titanates of mantle origin are of considerable interest because of their geochemical and petrological significance for various processes in the upper mantle. They have been suggested to be indicators for mantle metasomatism and offer potential repositories for high field-strength elements (HFSE), large-ion lithophile elements (LILE), and light rare earth elements (LREE) in the mantle (e.g., Haggerty 1983, 1991; Wang et al. 1999). Consequently, they may have great impact on the liberation or sequestration of these elements during partial melting of the mantle (e.g., Jones 1989). Titanates in subducted slabs (Ryerson and Watson 1987; Brenan et al. 1994), that remain as residual phases in source regions (Foley and Wheller 1990), or as form of metasomatic precipitates (Wang et al. 1999) have been inferred to play essential roles in generating one of the geochemical characteristics of island arc basalts (IAB), the depletion of HFSE relative to LILE and REE. Moreover, the

structures of titanates have been shown to be excellent indicators of high-pressure silicate isomorphs and hence may predict silicate phases that occur in the Earth's deep interior (e.g., Finger and Hazen 1991).

Through study of mantle-derived pyrope crystals and their included minerals from Garnet Ridge, Arizona, we found a titanate that appeared to be chemically unique. We take pleasure in naming this new mineral in honor of Professor Ian S. E. Carmichael in recognition of his numerous contributions to mineralogy and petrology, especially his studies of iron-titanium oxides from volcanic and mantle settings. The mineral and the name were approved by the Commission on New Minerals and Mineral Names, IMA. Because the original type crystal upon which the single-crystal XRD study was conducted was lost during an attempt to obtain powder XRD data, a co-type specimen still in its pyrope matrix is preserved in the National Museum of Natural History, Smithsonian Institution (catalogue number NMNH 172011.)

### OCCURRENCE AND PETROGENESIS

Garnet Ridge is one of seven localities for ultramafic diatremes in the Navajo volcanic field on the Colorado Plateau

\* Present address: Center for High Pressure Research, Department of Geosciences, State University of New York at Stony Brook, Stony Brook, New York 11794-2100. E-mail: lipwang@notes.cc.sunysb.edu

(e.g., McGetchin and Silver 1970). There are four irregularly shaped pipes cropping out within Jurassic sandstone at this locality (Hunter and Smith 1981). The host rock of the diatremes consists of serpentized ultramafic microbreccias containing comminuted crustal rocks and mantle xenoliths with related xenocrysts such as olivine, pyroxene, and garnet. Carmichaelite occurs as inclusions in three red or purple pyrope crystals collected from surface concentrates. These pyrope crystals also contain inclusions of rutile, srilankite, spinel, minerals of the crichtonite group, and olivine. Garnets of similar composition (not containing carmichaelite) from the same locality contain the following additional included phases: clinopyroxene, orthopyroxene, amphibole, phlogopite, titanian clinohumite, titanian chondrodite, chlorite, chlorapatite, ilmenite, magnesite, dolomite, and calcium carbonate (McGetchin et al. 1970; Hunter and Smith 1981; Smith 1987; Wang et al. 1999).

The new titanate mineral is completely included in its pyrope host, and in no case is it associated with cracks. We therefore conclude that it is part of a primary mineral assemblage and hence of mantle origin. Wang et al. (1999) inferred that the pyrope hosts formed during a spinel to garnet lherzolite transition in the presence of a fluid/melt phase that was highly enriched in incompatible elements (HFSE and LILE) and volatiles ( $\text{CO}_2$  and  $\text{H}_2\text{O}$ ). They concluded that carmichaelite and the other titanate inclusions were epitaxially precipitated in pyrope crystals from the metasomatic fluid/melt phase. Based on the foregoing study and the  $\text{Cr}_2\text{O}_3$  contents (3.8–5.1 wt%) of the pyrope hosts that contain carmichaelite, we estimate that it formed at temperatures of 650–750 °C and pressures of 20–25 kbar.

### PHYSICAL AND OPTICAL PROPERTIES

The anhedral to subhedral carmichaelite crystals occur, in most cases, in contact with rutile and occasionally with srilankite. Only one crystal of dimensions ca.  $20 \times 20 \times 30 \mu\text{m}^3$  was found as a single-phase inclusion. After the optical and chemical analyses were completed, the crystal was extracted from the pyrope host (GRPy-40) for IR and single-crystal X-ray study. The crystals are generally elongated in shape and  $\leq 30 \mu\text{m}$  in longest dimension (Fig. 1). They are translucent under high magnification. The crystals are cinnamon brown in color with a weak pleochroism when viewed with transmitted light, but the separated crystal appeared black when viewed with a binocular microscope.

The small size of carmichaelite crystals and their very high refractive indices [ $\sim 2.5$ , calculated from Mandarino (1981) assuming zero compatibility] made the determination of physical and optical properties difficult. The crystals have the same polishing quality as adjacent rutile, and we therefore infer that the two minerals have about the same Mohs hardness of  $\sim 6$ . The luster is metallic, and the fracture is brittle. No cleavage or twinning was observed. The calculated density is  $4.13 \text{ g/cm}^3$ . The reflected light is gray to white, and the reflectivity of the new mineral for normal incidence ( $R \sim 18\%$ ) is less than that of rutile and minerals of the crichtonite group but greater than those of geikielite and spinel. The estimated refractive index ( $2.0 < n < 2.9$ ) for carmichaelite based on this observation is consistent with the above calculated value. Its strong absorption prevents measurement of optical orientation and 2V.

### MINERAL CHEMISTRY

Chemical analyses of carmichaelite were done with a four-spectrometer Cameca Camebax electron microprobe using a typical acceleration voltage of 15 kV and a focused beam with a current of 10 nA. Counting times of 30 s or a total of 40 000 counts were used for all elements in both the standards and carmichaelite. All standards used were synthetic, and these included rutile (Ti), uvarovite (Cr), spinel (Al), ilmenite (Fe), geikielite (Mg),  $\text{V}_2\text{O}_5$  (V), and  $\text{Nb}_2\text{O}_5$  (Nb). Geikielite was also used as a standard for the direct determination of oxygen content with the electron microprobe. No other elements with atomic number greater than eight were detected in significant amounts by microprobe wavelength scans. The analytical data were corrected using the Cameca PAP program. Analyses of V have been corrected for the  $\text{TiK}\beta$  contribution to the  $\text{VK}\alpha$  peak by subtracting 0.0035·Ti wt% from the apparent V wt% of the carmichaelite crystals (Wang et al. 1999). Six grains of carmichaelite were analyzed. Five of these grains coexist with rutile and the other is an isolated crystal. This single crystal was also analyzed for oxygen. The normalization of its composition (including oxygen) to one total cation (excluding H) gives the number of oxygen atoms as 1.993(9), yielding cation:oxygen ratio of 1:2. Subsequently,  $\text{H}_2\text{O}$  concentrations were calculated based on charge balance and stoichiometry (i.e., cation:oxygen atoms = 1:2) for analyses of all grains. The average composition of each grain along with the composition of its pyrope host is listed in Table 1.

Carmichaelite in the same pyrope host (e.g., GRPy-40) has a uniform composition, and the mineral is chemically distinct from other titanates that occur as inclusions in the same or similar pyrope crystals from the same locality. The coexisting chromian rutile, to which it is most nearly alike, has only 5–6 wt%  $\text{Cr}_2\text{O}_3$ . Minerals of the crichtonite group contain amounts of  $\text{Cr}_2\text{O}_3$  similar to that of carmichaelite, but the former have significant concentrations of Ca, Sr, Ba, La, and Zr that allow them to be distinguished from carmichaelite (Wang et al. 1999). Similar differences exist between carmichaelite and other (K, Ba)-bearing titanates such as redledgeite (Gatehouse et al. 1986), priderite, jeppeite, yimengite, and hawthorneite (Haggerty 1991). The distribution coefficients of Cr/Al and Fe/Mg between carmichaelite and host pyrope, defined as  $(\text{Cr}/\text{Al})_{\text{cm}}/(\text{Cr}/\text{Al})_{\text{pp}}$  and  $(\text{Fe}/\text{Mg})_{\text{cm}}/(\text{Fe}/\text{Mg})_{\text{pp}}$ , are calculated to be  $44 \pm 8$  and  $7.1 \pm 0.6$  ( $1\sigma$  uncertainties), respectively. These values are identical within uncertainties to those between minerals of the crichtonite group and host pyrope (Wang et al. 1999). The carmichaelite grains in sample GRPy-40 have much lower Ti/Nb ratios than bulk silicate Earth (McDonough and Sun 1995). Compared to other titanate inclusions in the same pyrope host, carmichaelite crystals have Ti/Nb ratios lower than crichtonite, but higher than rutile (Wang et al. 1999).

### INFRARED SPECTROSCOPY

An infrared (IR) spectrum was obtained in the near IR region ( $1800\text{--}9000 \text{ cm}^{-1}$ ) from the extracted carmichaelite grain (Grain No. 1 in GRPy-40) using a Nicolet 60-SX Fourier transform infrared spectrometer equipped with an InSb detector. The sample, about  $20 \mu\text{m}$  thick, was placed on a  $25 \mu\text{m}$  aper-

ture. However, the aperture was not completely covered by the crystal due to the irregular shape and small size of the sample. The data were collected using a micro-chamber and averaged over 4096 scans at  $2\text{ cm}^{-1}$  resolution. Un-polarized light was perpendicular to the polished surface of carmichaelite (Fig. 1b). There is one main peak (perhaps with multiple components) centered at  $\sim 3330\text{ cm}^{-1}$  with a small shoulder at  $\sim 3580\text{ cm}^{-1}$  (Fig. 2). Both peaks are in the O-H stretching region and are tentatively assigned to structural OH. The concentration of OH is estimated to be  $\sim 5\text{--}6\text{ wt}\%$   $\text{H}_2\text{O}$ , assuming an absorptivity similar to that of the hydrous component (OH) in rutile (Lc; Hammer and Beran 1991). This estimate is consistent with the  $\text{H}_2\text{O}$  contents deduced from microprobe analyses (Table 1). There is, however, a baseline problem, probably arising from diffraction, which may affect the shape of the  $3330\text{ cm}^{-1}$  peak.

### X-RAY CRYSTALLOGRAPHY

Precession photographs of the extracted crystal (Grain No. 1 in GRPy-40) showed sharp reflections, suggesting that it was a well-crystallized single crystal. The unit-cell parameters and space group could not be obtained by this method, however, due to the small number of observed reflections. The crystal was then studied using an Enraf-Nonius CAD4 four-circle

serial diffractometer and later a standard Siemens SMART CCD-based diffractometer. The results showed that carmichaelite is monoclinic, with the probable space group  $P2_1/c$ . The unit-cell parameters obtained in both studies are similar, but the values obtained from the CCD-based diffractometer are systematically greater than those from the serial diffractometer by ca. 0.2%. The parameters from the CCD-based diffractometer are  $a = 7.706(1)$ ,  $b = 4.5583(6)$ ,  $c = 20.187(3)\text{ \AA}$ , and  $\beta = 92.334(2)^\circ$ , whereas the serial diffractometer gave  $a = 7.686(3)$ ,  $b = 4.5492(3)$ ,  $c = 20.151(2)\text{ \AA}$ , and  $\beta = 92.30(2)^\circ$ . The first set is to be preferred because of the superior sensitivity and resolution of the CCD detector relative to conventional scintillation counters, an advantage of great importance when working with exceedingly small crystals (Burns 1998).

Although data sets obtained from two different diffractometers yielded consistent results, they must be viewed with some caution. The most probable cell parameters, crystal system, and lattice type of the crystal were done automatically according to standard algorithms. However, during the search phase of the procedure, a superstructure that is defined by a small number of very weak reflections may easily be overlooked, and the potential for such an error increases in cases where all reflections are weak owing to small crystal size. It is not inconceivable, therefore, that the cell parameters and space group

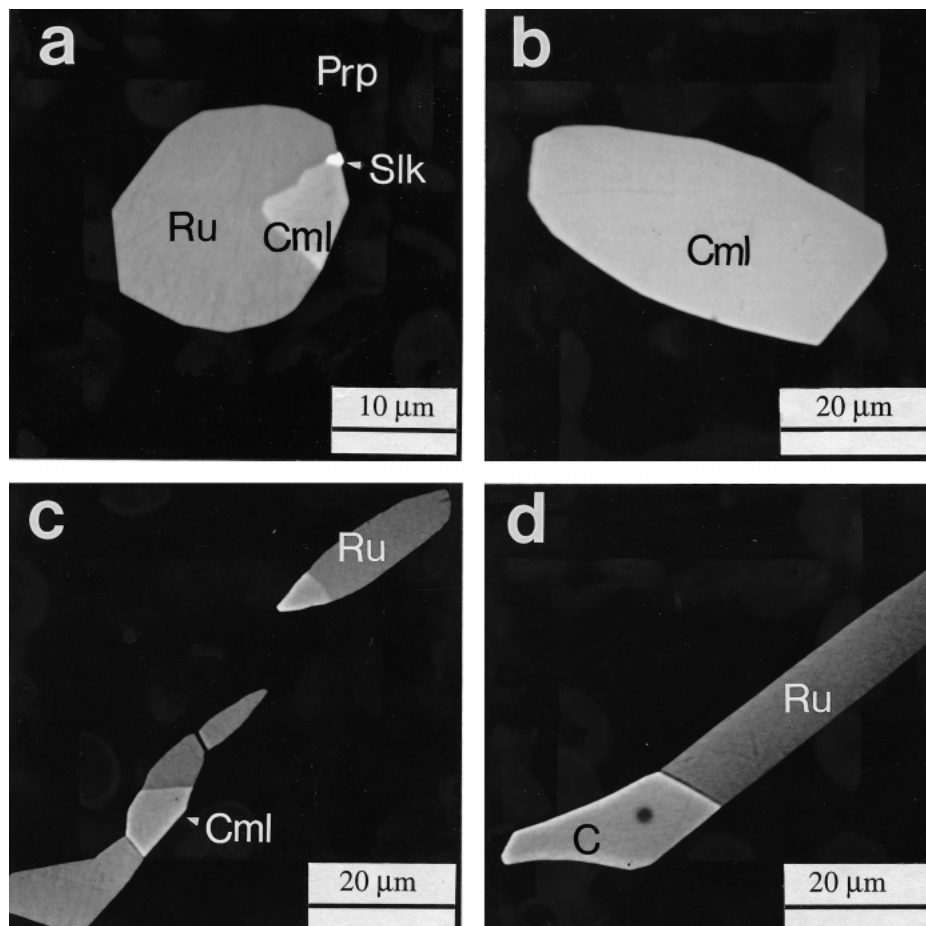


**FIGURE 1.** Backscattered electron (BSE) images of carmichaelite and coexisting inclusions in host pyrope (Prp): (a) carmichaelite (Cml) coexisting with rutile (Ru) and srilankite (Slk) in GRPy-39; (b) single-phase carmichaelite crystal in GRPy-40; (c and d) carmichaelite coexisting with rutile in GRPy-41.

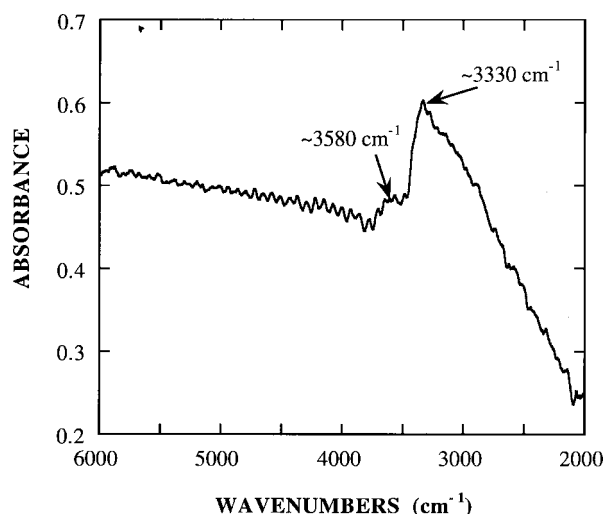


FIGURE 2. Infrared spectrum of carmichaelite showing the presence of OH groups. The oscillations are interference fringes.

symmetry reported here for carmichaelite are those of a subcell of the true cell.

X-ray intensities were collected with the CCD-based diffractometer and MoK $\alpha$  radiation at 295( $\pm$ 2) K. A full sphere of data consisting of a total of 2132 frames were collected with a scan width of 0.3° in  $\omega$  and an exposure time of 360 s/frame. The frames were integrated with the Siemens SAINT software package with a narrow frame algorithm. The integration of the data using a monoclinic unit cell yielded a total of 6717 reflections to a maximum 2 $\theta$  value of 58.5° of which 1586 were independent. Analysis of the data showed negligible decay during data collection. The data were corrected for Lorentz and polarization effects.

An attempt to obtain powder X-ray diffraction data on the extracted crystal with a Gandolfi camera, as was requested by a reviewer of the IMA submission, failed because the sample was lost during mounting. Such data could not be obtained on small samples included in garnet due to their small sizes and the resulting weak diffraction intensities. We have therefore calculated a powder pattern using a program provided by Scintag, Inc. (Cupertino, CA) based on the results of the crystal structure analysis (Table 2). The relative intensities from the single-crystal data were adjusted by taking reflection multiplicity into account; they are in excellent agreement with those of the calculated powder pattern.

### STRUCTURE SOLUTION AND REFINEMENT

The structure was solved and refined in the space group  $P2_1/c$  using the Enraf-Nonius crystallographic software system MOLEN. MULTAN 11/82 revealed the locations of all eight cation (M1-M8) and eleven anion sites, with only one cation site (M1) on a special position. Since the anion sites proved to be fully occupied, yielding a total of 44 oxygen atoms per cell, and since the chemical analysis shows unequivocally that the cation:oxygen ratio is 1:2 within analytical error (Table 1), the number of cations per cell is fixed at 22. The eight cation sites per cell will accommodate 30 atoms, and thus some of these sites must be partially occupied. Refining this model using, initially, the scattering curve of titanium for all cation sites and adjusting their site occupancies by trial-and-error to give reasonable refined isotropic displacement factors for all atoms, the "all titanium model" refinement converged at an unweighted residual of 0.080. During this process, two problems appeared involving the anion displacement factors: their behavior was acutely sensitive to the exact values used for the site occupancies at the cation sites and they would only refine to reasonable values if all reflections above 45.0° 2 $\theta$  were excluded from the

TABLE 1. Electron microprobe analyses of carmichaelite and host pyrope

Host no.	39	40	2	3	41		39	40	41	
Grain no.	1	1*			1	2	host	host	host	
No. of analyses	6	14	8	6	3	4	7	8	9	
TiO <sub>2</sub>	63.13	61.91	61.29	61.80	62.40	62.44	SiO <sub>2</sub>	41.83	41.87	41.55
Cr <sub>2</sub> O <sub>3</sub>	17.95	17.98	17.34	18.10	19.52	19.67	TiO <sub>2</sub>	0.06	0.10	0.11
Al <sub>2</sub> O <sub>3</sub>	1.81	2.06	2.11	2.21	1.52	1.58	Al <sub>2</sub> O <sub>3</sub>	20.83	20.48	19.92
FeO†	7.06	7.85	8.47	8.10	7.15	7.05	Cr <sub>2</sub> O <sub>3</sub>	3.81	4.64	5.08
MgO	2.82	2.74	2.94	2.81	2.71	2.80	MgO	20.05	19.74	20.07
Nb <sub>2</sub> O <sub>5</sub>	0.02	0.78	0.58	0.81	0.04	0.03	FeO†	8.30	7.49	7.58
V <sub>2</sub> O <sub>5</sub> ‡	0.87	1.00	1.00	0.96	0.67	0.75	CaO	4.52	5.47	4.92
H <sub>2</sub> O§	5.58	5.75	5.95	5.88	5.66	5.72	MnO	0.41	0.42	0.35
Total	99.24	100.07	99.68	100.67	99.67	100.04		99.81	100.21	99.58
<b>Formulae normalized to 1 cation</b>						<b>Formulae normalized to 8 cations</b>				
Ti	0.636	0.621	0.616	0.616	0.628	0.626	Si	3.002	3.000	2.996
Cr	0.190	0.190	0.183	0.190	0.207	0.207	Ti	0.003	0.005	0.006
Al	0.029	0.032	0.033	0.035	0.024	0.025	Al	1.762	1.729	1.692
Fe	0.079	0.088	0.095	0.090	0.080	0.079	Cr	0.216	0.263	0.290
Mg	0.056	0.054	0.059	0.055	0.054	0.056	Mg	2.146	2.108	2.157
Nb	0.000	0.005	0.003	0.005	0.000	0.000	Fe	0.498	0.449	0.457
V	0.009	0.011	0.011	0.010	0.007	0.008	Ca	0.348	0.420	0.380
OH§	0.498	0.512	0.532	0.520	0.506	0.510	Mn	0.025	0.026	0.021

Note: Samples are GRPy-39 to GRPy-41.

\* Isolated crystal of carmichaelite; the other grains are all in contact with rutile. The measured oxygen content is 39.79 wt%.

† All Fe as FeO.

‡ Corrected for Ti interference; all V as V<sub>2</sub>O<sub>5</sub>.

§ OH calculated as Cr + Al + V + 2 Fe + 2 Mg-Nb.

**TABLE 2.** Calculated X-ray powder diffraction data for carmichaelite

$I_{\text{meas}}^*$	$I_{\text{calc}}^\dagger$	$d_{\text{calc}}$ (Å)	$h$	$k$	$l$
82	94	3.773	0	1	3
100	100	2.842	1	1	5
63	70	2.664	2	1	3
26	26	2.512	3	0	2
19	21	2.483	2	0	6
12	15	2.425	1	0	8
5	7	2.279	0	2	0
12	15	2.214	3	1	1
23	22	2.200	3	1	2
27	22	2.180	2	1	6
22	20	2.141	1	1	8
10	11	1.986	3	1	5
62	54	1.688	3	2	2
49	44	1.679	2	2	6
46	44	1.661	1	2	8
34	34	1.648	1	1	11
15	17	1.536	4	1	7
24	20	1.456	5	0	4
12	13	1.451	5	1	1
20	18	1.422	4	0	10
12	11	1.406	1	0	14
10	11	1.402	1	3	5
13	15	1.390	2	1	13
13	14	1.379	2	3	3
13	16	1.366	4	1	9
5	5	1.303	3	3	1
5	7	1.152	1	3	11
9	8	1.140	0	4	0
12	11	1.100	6	2	4
6	6	1.090	4	2	12

\* Intensities from single-crystal XRD data corrected for line multiplicity.

† Intensities for the powder pattern calculated from the carmichaelite structure model.

refinement. With an observed reflection threshold of  $1 \sigma_r$ , this left only 338 reflections available for the refinement of the structure. The reflection weights used were of the form  $4F_{\text{obs}}^2/\sigma^2(F_{\text{obs}}^2)$ .

Using as guides the calculated mean bond distances and the approximate X-ray scattering powers at the cation sites deduced from the "all titanium model", the next step was to attempt to fit the cation contents of the unit cell calculated from the chemical analysis (Table 1) to the eight available cation sites. This process was complicated by four factors: (1) the similarity in cation radii and X-ray scattering powers of Ti, V, Cr, and Fe;

(2) the existence of multiple possible valence states for Fe and perhaps V; (3) partial occupancy of the cation sites M5, M6, M7, and M8 owing to improbably short cation-cation distances less than 2.5 Å; and (4) the substandard quality of the data. Many solid solution models were tested, all being judged by the same three criteria, namely, minimization of the residual, reasonableness of the refined cation and anion displacement factors, and ability to accommodate the full cation contents of the unit cell in a crystal-chemically reasonable way. The model that best met these criteria converged at residuals of 0.074 (unweighted), 0.062 (weighted), and 0.270 (all reflections including those that were treated as unobserved) and is the one reported in Table 3. Other variants of the solid solution model and models that are significantly different, e.g., those involving (Ti, Al) on M1 and (Ti, Cr) on M2, M3, and M4, are also possible, although they gave worse refinement results when tested. The cation site assignments in Table 3 are therefore provisional, pending the future acquisition of better-quality intensity data.

In addition to the refined atomic parameters in Table 3, Table 4<sup>1</sup> contains the observed and calculated structure factors and Table 5 selected interatomic distances. Empirical bond-valence sums calculated from the observed cation-oxygen distances and the constants of Brese and O'Keeffe (1991) are listed in Table 6.

## STRUCTURE DESCRIPTION AND DISCUSSION

### Overview

The structure of carmichaelite consists of stacked chains of cation octahedra in an array of hexagonal closest-packed oxygen atoms, the hcp layers being parallel to (010). The asymmetric unit contains eight distinct six-coordinated cation sites, of which the M1 atoms are located on inversion centers and

<sup>1</sup>For a copy of Table 4, document item AM-00-044, contact the Business Office of the Mineralogical Society of America (see inside front cover of recent issue) for price information. Deposit items may also be available on the American Mineralogist web site (<http://www.minsocam.org>).

**TABLE 3.** Atomic parameters and site contents for carmichaelite

Site	$x$	$y$	$z$	$B_{\text{iso}}$ (Å <sup>2</sup> )	Site occupancies	Mult
M1	1/2	0	0	1.3(1)	1.00 Ti	2
M2	0.0562(5)	0.007(1)	0.3113(2)	0.30(6)	0.94 Ti + 0.06 V	4
M3	0.4128(4)	0.992(1)	0.3691(2)	0.34(7)	0.975 Ti + 0.025 Nb	4
M4	0.1328(5)	0.999(1)	0.9448(2)	0.57(7)	1.00 Ti	4
M5	0.3271(5)	0.000(1)	0.7396(2)	0.65(8)	0.775 Cr	4
M6	0.2187(7)	0.016(2)	0.5747(3)	0.7(1)	0.27 Cr + 0.17 Fe + 0.18 Al	4
M7	0.2799(63)	0.040(10)	0.2046(27)	0.6(9)	0.14 Mg	4
M8	0.2375(10)	0.021(2)	0.1051(4)	0.5(1)	0.31 Fe + 0.16 Mg	4
O1	0.703(2)	0.293(3)	0.4866(8)	2.5(3)		4
O2	0.259(2)	0.255(2)	0.8074(7)	1.1(2)		4
O3	0.173(2)	0.283(3)	0.1637(8)	2.1(3)		4
O4	0.807(2)	0.283(3)	0.1193(8)	1.7(3)		4
O5	0.624(2)	0.215(3)	0.3502(7)	0.9(2)		4
O6	0.066(2)	0.252(3)	0.0206(9)	2.6(3)		4
O7	0.355(2)	0.286(3)	0.4372(8)	2.3(3)		4
O8	0.523(2)	0.253(3)	0.2140(9)	2.7(3)		4
O9	0.889(2)	0.240(3)	0.2564(7)	0.9(2)		4
O10	0.986(2)	0.233(3)	0.3930(7)	1.2(3)		4
O11	0.436(2)	0.283(3)	0.0731(8)	2.3(3)		4

**TABLE 5.** Selected interatomic distances (Å)

M1-O1	1.86(3)×2	M5-O2	1.89(2)	M8-O1	2.19(3)
M1-O7	1.92(3)×2	M5-O3*	2.14(3)	M8-O3*	1.77(3)
M1-O11	2.04(3)×2	M5-O5*	2.11(2)	M8-O5*	1.95(2)
mean	1.94	M5-O8*	1.86(3)	M8-O6*	2.36(3)
		M5-O8*	1.97(3)	M8-O10*	2.17(3)
M2-O2	1.91(2)	M5-O9	2.00(3)	M8-O11	2.07(3)
M2-O3*	2.12(3)	mean	2.00	mean	2.09
M2-O4	2.00(3)				
M2-O9	1.98(2)	M6-O1	1.99(3)		
M2-O9	1.89(2)	M6-O3*	2.06(3)	M5-M7	2.58(7)
M2-O10*	2.04(3)	M6-O5*	2.17(2)	M5-M7	2.24(6)
mean	1.99	M6-O6*	1.90(2)	M6-M8	2.53(2)
		M6-O10*	2.07(2)	M6-M8	2.20(1)
M3-O2	2.04(2)	M6-O11	1.91(3)	M7-M8	2.03(7)
M3-O4	1.97(3)	mean	2.02		
M3-O5*	1.97(2)				
M3-O7	1.98(3)	M7-O2	2.29(7)	O1-O7	2.51(4)
M3-O8*	2.08(3)	M7-O3*	1.59(7)	O2-O4	2.63(3)
M3-O11	1.87(3)	M7-O5*	2.01(7)	O3*-O5*	2.53(2)
mean	1.99	M7-O8*	2.11(7)	O3*-O9	2.69(3)
		M7-O8*	2.55(7)	O3*-O10*	2.63(3)
M4-O1	2.06(2)	M7-O9	2.06(7)	O5*-O8*	2.69(3)
M4-O4	1.90(3)	mean	2.10	O5*-O11	2.56(3)
M4-O6*	2.00(3)			O6*-O6*	2.60(4)
M4-O6*	2.05(3)			O6*-O10*	2.63(3)
M4-O7	1.99(3)				
M4-O10*	1.94(2)				
mean	1.99				

\* Probable (O, OH) sites.

**TABLE 6.** Bond-valence sums (valence units)

M1	4.38	M6	1.65	O3*	1.53	O8*	1.50
M2	3.80	M7	0.38	O4	2.08	O9	1.87
M3	3.88	M8	1.13	O5*	1.42	O10*	1.62
M4	3.79	O1	1.83	O6*	1.58	O11	1.95
M5	2.34	O2	1.85	O7	2.02		

Note: Bond valences were calculated using the parameters of Brese and O'Keeffe (1991).

\* Probable (O, OH) sites.

the other sites on general positions (Table 3). Four of these cation sites (M5, M6, M7, and M8) are partially occupied, as indicated by short cation-cation distances and their site occupancies (Table 5). Hence, pairs of M5-M7 and M6-M8 sites can each accommodate a maximum of four atoms per pair. All anions are three-coordinated (excluding H) based on such partial occupancies. The basic building block of the carmichaelite structure are the units of five edge-sharing octahedra (Fig. 3a), adjacent blocks being connected to each other by edge-sharing to form chains of octahedra. Three such chains are then connected by edge-sharing between M7 and M8 octahedra to form a triple chain. Because of very short metal-metal distances (2.03 Å, Table 5), M7 and M8 sites cannot both be occupied locally, and the triple chains therefore exist only as a statistical average feature of the structure. In the third dimension, the triple chains are offset from one another along [010], creating narrow zigzag tunnels along [100] (Figs. 3b and 3c). In this way, the structure resembles those of rutile and related structures and those of the Mn(IV) oxides (Burns and Burns 1979; Bursill 1979; Finger and Hazen 1991).

### Octahedral chain and related compounds

The basic structural unit of five edge-sharing octahedra in carmichaelite (Fig. 3a) is the same as that found in the struc-

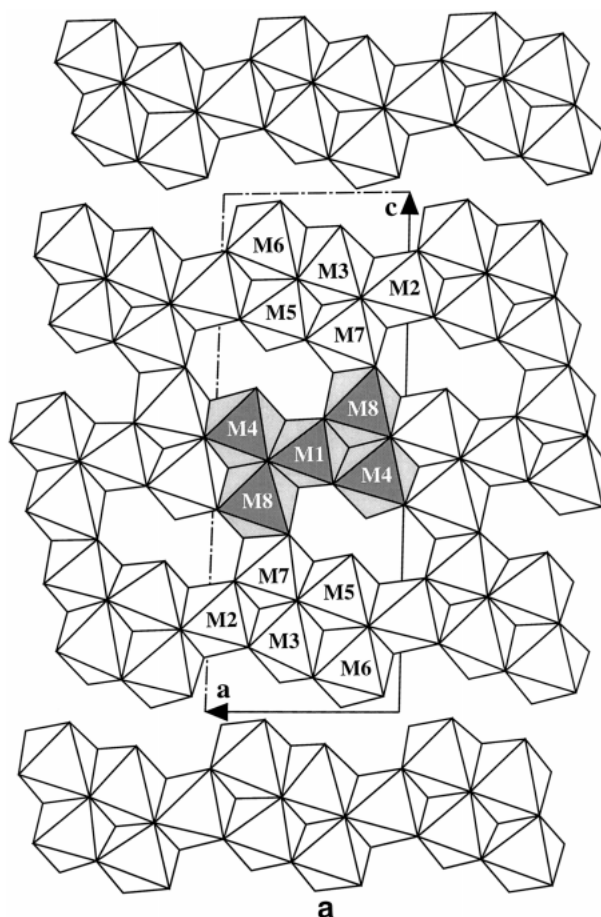
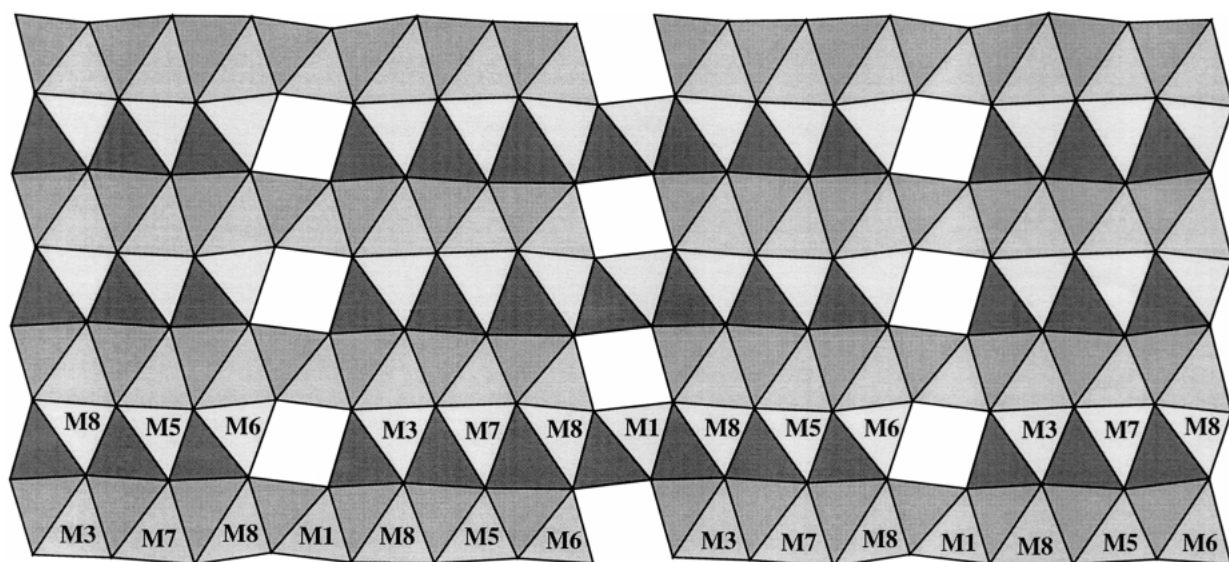


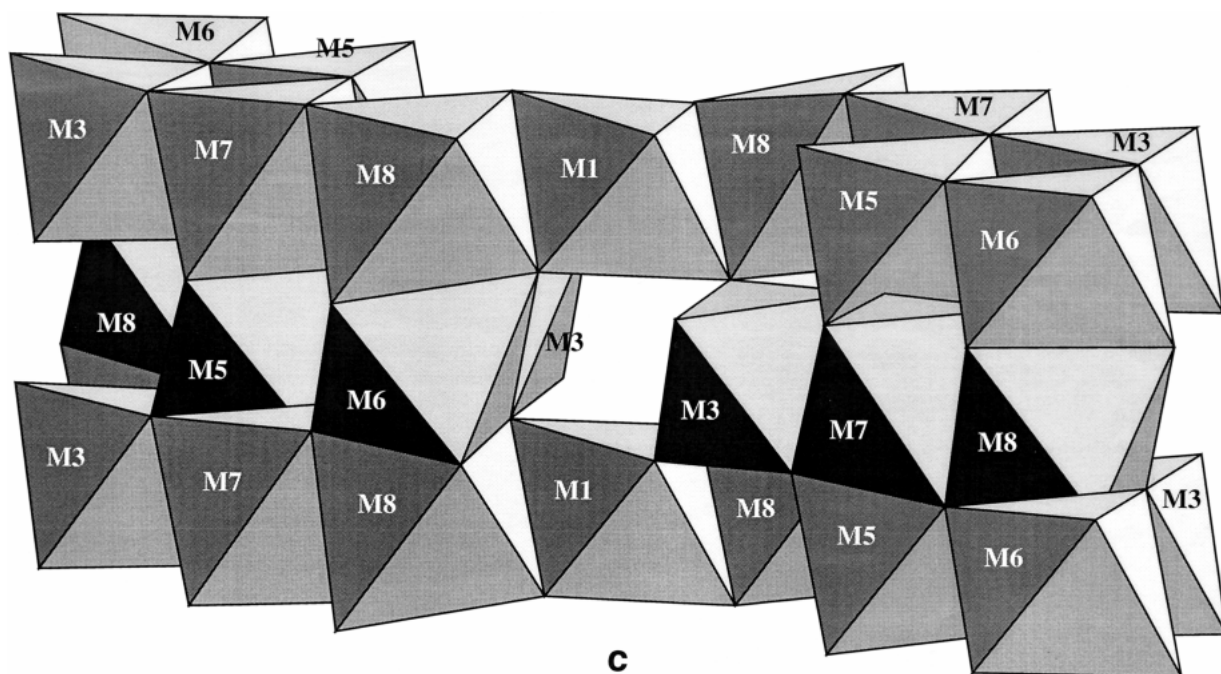
**FIGURE 3.** The structure of carmichaelite. (a) An octahedral layer in carmichaelite projected down *b* from  $y = 1/8$  to  $7/8$ . The unit cell is outlined. Shaded octahedral sites form the five-membered cluster building block.

*Figure continued next page*

ture of leucophoenicite (Moore 1970), olivine, and members of the humite group (Papike and Cameron 1976). However, the octahedral five-membered clusters are arranged differently to form octahedral chains in these minerals. In leucophoenicite and olivine, two clusters are connected by sharing two and one octahedra, respectively. In some members of the humite group (clinohumite, humite and chondrodite), they are connected by edge-sharing between two octahedra. Five-membered clusters of octahedra are also found in the  $V_3O_5$  structure, where they are arranged similarly to those in leucophoenicite (Åsbrink 1980; Hong and Åsbrink 1982). In this regard, some similarity exists between carmichaelite and natural and synthetic members of "Andersson phases" as the latter structures contain  $V_3O_5$  layers (Flörke and Lee 1970; Grey et al. 1973; Medenbach and Schmetzer 1978; Bernhardt et al. 1983). On the other hand, the carmichaelite structure appears to bear no close relationship (aside from its structural tunnels) to the structures of some well-known titanates such as  $TiO_2$  polymorphs, pseudorutile (Grey



b



c

FIGURE 3—continued. (b) Seven octahedral layers projected down a, showing multiple tunnels and the offset of chains along [010]. (c) Three octahedral layers viewed approximately along a, i.e., parallel to the hcp O layers, showing the three-dimensional arrangement of octahedra.

and Reid 1975), members of the crichtonite group (e.g., Grey et al. 1976), and the synthetic high-pressure Ti-Cr oxyhydroxides (Herrero-Fernandez et al. 1984).

### The presence of OH and chemical formula

The initial microprobe analyses with assumed O of carmichaelite yielded low totals (i.e., < 95%), even after assuming all Fe to be Fe<sup>3+</sup>. When O was directly measured, the analyses gave acceptable totals (i.e., ~99%), indicating the presence of a hydrous component in carmichaelite. The IR data support this conclusion (Fig. 2). The empirical bond-valence calculations for all non-H atoms show that bond-valence sums to all O anions are greater than 1.40 (Table 6), precluding the presence of H<sub>2</sub>O groups and implying the presence of OH. However, the large breadth of 3330 cm<sup>-1</sup> band extending to lower wavenumber (Fig. 2) is at odds with the sharp OH bands in other titanates, such as rutile. This could be due to a cascade of overlapping OH peaks in the frequency range of 2000–3000 cm<sup>-1</sup>. The short anion-anion distances (Table 5) imply low frequencies for OH bands, and distances of 2.53–2.69 Å would yield frequencies in the range of 2310–3210 cm<sup>-1</sup> (Libowitzky 1999). A study using polarized beam or at low temperatures will help resolve the ambiguities. Bands at higher frequencies (i.e., 3580 cm<sup>-1</sup>) could be resulted from O-H···O with larger anion-anion distances. For instance, O6, one of probable (O, OH) sites, has a distance of 3.05 Å to O1, which implies an OH band at ~3570 cm<sup>-1</sup>.

The bond-valence calculations show that some anion sites have sums much less than 2 (Table 6), suggesting O and OH mixing on these sites. The O3, O5, O6, O8, and O10 sites have sums close to 1.5 (average = 1.53 ± 0.08), suggesting that approximately half of each site is statistically occupied by OH and the other half by O. The partially occupied cation sites are coordinated by more OH groups than the fully occupied ones (Table 5). The H atoms are satisfying the bond-valence requirements of the anions when the metal atoms are absent from the cation sites. The total amount of OH present in the unit cell can be estimated assuming an ideal bond-valence sum of 2 for each anion site. Since the bond-valence calculations yielded an average valence of 1.75 for all anions (Table 6), a total of 11 H atoms per unit cell is implied (corresponding to 5.8 wt% H<sub>2</sub>O), in excellent agreement with the value deduced from microprobe analyses (Table 1). All H-bearing anions are inferred to participate in H-bonding, a conclusion based on their relatively short anion-anion distances (Table 5). Hence, the carmichaelite structure is stabilized by the H bonds, most of which are aligned probably along the edges of vacant cation sites.

The chemical formula for carmichaelite is complicated by the uncertainties in the absolute water content, the Fe<sup>3+</sup>/Fe<sup>2+</sup> ratio, and solid solutions. If all Fe is assumed to be Fe<sup>2+</sup>, the calculated water content is ~11 H per unit cell or 5.8 wt% H<sub>2</sub>O (Table 1), corresponding to the empirical formula Mg<sub>0.056</sub>Fe<sub>0.085</sub><sup>2+</sup>Cr<sub>0.194</sub>Al<sub>0.030</sub>Ti<sub>0.624</sub>V<sub>0.009</sub>Nb<sub>0.002</sub>O<sub>1.488</sub>(OH)<sub>0.512</sub>. If all Fe is assumed to be Fe<sup>3+</sup>, the calculated water content is ~9 H per unit cell or 4.8 wt% H<sub>2</sub>O, corresponding to the empirical formula Mg<sub>0.056</sub>Fe<sub>0.085</sub><sup>3+</sup>Cr<sub>0.194</sub>Al<sub>0.030</sub>Ti<sub>0.624</sub>V<sub>0.009</sub>Nb<sub>0.002</sub>O<sub>1.572</sub>(OH)<sub>0.428</sub>. In both cases, the chemical analyses yield acceptable totals. Although the former is more consistent with the structure analy-

sis, Fe may be present in two valence states in carmichaelite, but the proportions could not be determined. The OH content is related to elements that have a valence state different from Ti (i.e., Cr, Mg, and Al) as some H atoms enter the carmichaelite structure through coupled substitutions such as H<sup>+</sup> + Cr<sup>3+</sup> for Ti<sup>4+</sup>. The solid-solution model (Table 3) indicates that Ti and Cr are ordered in the structure. It would thus be possible to describe carmichaelite with the ideal formula of Cr<sub>4</sub>Ti<sub>7</sub>O<sub>18</sub>(OH)<sub>4</sub>, assuming that Nb and V substitute for Ti, and Mg, Al and Fe substitute for Cr. But the solid-solution model is only a tentative approximation, and we therefore prefer to use the simplified formula MO<sub>2-x</sub>(OH)<sub>x</sub>, where M includes Ti, Cr, Fe, Mg, and Al.

### Implications for phase equilibria and geochemistry

Extensive phase-equilibria studies are available for the systems TiO<sub>2</sub>-Cr<sub>2</sub>O<sub>3</sub> (e.g., Andersson et al. 1959; Flörke and Lee 1970; Gibb and Anderson 1972) and Cr<sub>2</sub>O<sub>3</sub>-Fe<sub>2</sub>O<sub>3</sub>-TiO<sub>2</sub> (e.g., Grey and Reid 1972; Grey et al. 1973; Fotiev et al. 1981). At ambient pressure, these authors synthesized the “Andersson phases”, which have the general formula Cr<sub>2</sub>Ti<sub>n-2</sub>O<sub>2n-1</sub> (where n = 6–9), and also compounds with the general formula (Cr,Fe)<sub>2</sub>Ti<sub>n-2</sub>O<sub>2n-1</sub> (where n = 3–5). The phase equilibria in these systems at high pressure and in the presence of H<sub>2</sub>O, which are of more geological importance, remain almost unvisited. Herrero-Fernandez et al. (1984) accidentally synthesized a series of Ti-Cr oxyhydroxides at 60 kbar and 1000 °C. Water was not included in the starting sample mixtures, but was inadvertently provided by the breakdown of the pressure medium pyrophyllite during experimental runs. These oxyhydroxides have the general formula Ti<sub>1-x</sub>Cr<sub>x</sub>O<sub>2-x</sub>(OH)<sub>x</sub> (where 0.05 ≤ x ≤ 0.30) and orthorhombic, distorted rutile-type structures, and demonstrate that water plays important role in the phase equilibria under consideration. The discovery of carmichaelite further points to the need for a systematic experimental study of the Cr<sub>2</sub>O<sub>3</sub>-Fe<sub>2</sub>O<sub>3</sub>-TiO<sub>2</sub>-H<sub>2</sub>O system at high pressures and temperatures.

Carmichaelite is a new member of a growing family of titanates derived from various ultramafic environments (Haggerty 1983, 1991; Wang et al. 1999). Its presence in pyrope crystals of peridotitic association suggests the involvement of a metasomatizing fluid/melt phase. The estimated formation conditions for carmichaelite (650–750 °C and 20–25 kbar) indicate a relatively cool source region. Hence, the carmichaelite inclusions most likely formed in a metasomatized mantle wedge overlying a subducted slab in which carmichaelite might serve as a potential repository for water. Because of the high concentrations of both Ti and Nb in carmichaelite (especially inclusions in GRPy-40; Table 1), it might be among the titanates responsible for HFSE depletion in island arc basalts (e.g., Foley and Wheller 1990; Wang et al. 1999). Messiga et al. (1999) reported the occurrence of peculiar Cr-Ti oxides in eclogites from the Monviso ophiolites (Western Alps, Italy) in association with chromite, rutile, magnesite, chloritoid, omphacite, talc and garnet. The chemical composition of the Cr-Ti oxides strikingly resembles to that of carmichaelite, although the content of some elements (i.e., Cr) might have been affected by the fluorescence of the adjacent chromite by Fe X-rays in the Cr-

Ti oxides. The formation conditions for these oxides were estimated to be  $620 \pm 50$  °C and 24 kbar, also consistent with those inferred for carmichaelite. Therefore, it seems likely that the Cr-Ti oxides reported by Messiga et al. (1999) are a further occurrence of carmichaelite. This finding suggests that carmichaelite could be one of the controlling minerals for HFSE inventory in subductive environments. Lastly, the structures of mantle-derived titanates have been suggested as indicators of high-pressure silicate isomorphs with  $^{61}\text{Si}$  (Finger and Hazen 1991). Thus, the presence of a high-pressure phase similar to carmichaelite may be proposed in the Si-Al-O-H system. The estimated formula would be close to  $\text{Al}_3\text{Si}_7\text{O}_{18}(\text{OH})_4$ , assuming that Si could substitute for Ti and Al for Cr and Fe in a carmichaelite-like structure. All Si would be six-coordinated in this phase, and it could be stable and present in the deep regions of the Earth's mantle.

### ACKNOWLEDGMENTS

We thank S. Dunn, S.C. Semken, and A. Zaman for their help in field work and the Navajo Nation for permission to collect samples. J.W. Kampf is thanked for obtaining X-ray intensity data on the CCD-based diffractometer in the Department of Chemistry, University of Michigan. Review comments from P.C. Burns, A.M. Hofmeister, R. Oberti, and an anonymous reviewer are greatly appreciated. This study was supported by NSF grants EAR 94-58368 and 97-25566; a research grant from NWT Geology Division of the Department of Indian Affairs and Northern Development, Canada; the Scott Turner Fund of the University of Michigan; and a research grant from the Geological Society of America. This is contribution No. 513 from the Mineralogical Laboratory, Department of Geological Sciences, University of Michigan.

### REFERENCES CITED

- Andersson, S., Sundholm, A., and Magnéli, A. (1959) A homologous series of mixed titanium chromium oxides  $\text{Ti}_{n-2}\text{Cr}_2\text{O}_{2n-1}$  isomorphous with the series  $\text{Ti}_n\text{O}_{2n-1}$  and  $\text{V}_n\text{O}_{2n-1}$ . *Acta Chemica Scandinavica*, 13, 989–997.
- Åsbrink, S. (1980) The crystal structure of and valency distribution in the low-temperature modification of  $\text{V}_3\text{O}_5$ : The decisive importance of a few weak reflexions in a crystal-structure determination. *Acta Crystallographica*, B36, 1332–1339.
- Bernhardt, H.J., Schmetzer, K., and Medenbach, O. (1983) Berdensinskiite,  $\text{V}_2\text{TiO}_5$ , a new mineral from Kenya and additional data for schreyerite,  $\text{V}_2\text{Ti}_3\text{O}_9$ . *Neues Jahrbuch für Mineralogie Monatshefte*, 110–118.
- Brenan, J.M., Shaw, H.F., Phinney, D.L., and Ryerson, F.J. (1994) Rutile-aqueous fluid partitioning of Nb, Ta, Hf, Zr, U and Th: Implications for high field strength element depletions in island-arc basalts. *Earth and Planetary Science Letters*, 128, 327–339.
- Brese, N.E. and O'Keeffe, M. (1991) Bond-valence parameters for solids. *Acta Crystallographica*, B47, 192–197.
- Burns, P.C. (1998) CCD area detectors of X-rays applied to the analysis of mineral structures. *Canadian Mineralogist*, 36, 847–853.
- Burns, R.G. and Burns, V.M. (1979) Manganese Oxides. In *Mineralogical Society of America Reviews in Mineralogy*, 6, 1–46.
- Bursill, L.A. (1979) Structural relationship between  $\beta$ -gallia, rutile, hollandite, psilomelane, ramsdellite and gallium titanate type structures. *Acta Crystallographica*, B35, 530–538.
- Finger, L.W. and Hazen, R.M. (1991) Crystal chemistry of six-coordinated silicon: A key to understanding the Earth's deep interior. *Acta Crystallographica*, B47, 561–580.
- Flörke, O.W. and Lee, C.W. (1970) Andersson Phasen, dichteste Packung und Wadsley Defekte im System Ti-Cr-O. *Journal of Solid State Chemistry*, 1, 445–453.
- Foley, S.F. and Wheller, G.E. (1990) Parallels in the origin of the geochemical signatures of island arc volcanics and continental potassic igneous rocks: The role of residual titanates. *Chemical Geology*, 85, 1–18.
- Fotiev, A.A., Surat, L.L., and Tret'yakov, A.I. (1981) Phase relationships in the  $\text{Al}_2\text{O}_3$ - $\text{Fe}_2\text{O}_3$ - $\text{TiO}_2$ - $\text{V}_2\text{O}_5$ ,  $\text{Cr}_2\text{O}_3$ - $\text{Fe}_2\text{O}_3$ - $\text{TiO}_2$ - $\text{V}_2\text{O}_5$ , and  $\text{Al}_2\text{O}_3$ - $\text{Cr}_2\text{O}_3$ - $\text{TiO}_2$ - $\text{V}_2\text{O}_5$  systems. *Russian Journal of Inorganic Chemistry*, 26, 739–743.
- Gatehouse, B.M., Jones, G.C., Pring, A., and Symes, R.F. (1986) The chemistry and structure of redlegite. *Mineralogical Magazine*, 358, 709–715.
- Gibb, R.M. and Anderson, J.S. (1972) The system  $\text{TiO}_2$ - $\text{Cr}_2\text{O}_3$ : Electron microscopy of solid solutions and crystallographic shear structures. *Journal of Solid State Chemistry*, 1, 445–453.
- Grey, I.E. and Reid, A.F. (1972) Shear structure compounds  $(\text{CrFe})_2\text{Ti}_{n-2}\text{O}_{2n-1}$  derived from the  $\alpha$ - $\text{PbO}_2$  structural type. *Journal of Solid State Chemistry*, 4, 186–194.
- (1975) The structure of pseudorutile and its role in the natural alteration of ilmenite. *American Mineralogist*, 60, 898–906.
- Grey, I.E., Reid, A.F., and Allpress, J.G. (1973) Compounds in the system  $\text{Cr}_2\text{O}_3$ - $\text{Fe}_2\text{O}_3$ - $\text{TiO}_2$ - $\text{ZrO}_2$  based on intergrowth of the  $\alpha$ - $\text{PbO}_2$  and  $\text{V}_3\text{O}_5$  structure types. *Journal of Solid State Chemistry*, 8, 86–99.
- Grey, I.E., Lloyd, D.J., and White, J.S., Jr. (1976) The structure of crichtonite and its relationship to senaite. *American Mineralogist*, 61, 1203–1212.
- Haggerty, S.E. (1983) The mineral chemistry of new titanates from the Jagersfontein kimberlite, South Africa: Implications for metasomatism in the upper mantle. *Geochimica et Cosmochimica Acta*, 47, 1833–1854.
- (1991) Oxide mineralogy of the upper mantle. In *Mineralogical Society of America Reviews in Mineralogy*, 25, 355–416.
- Hammer, V.M.F. and Beran, A. (1991) Variations in the OH concentration of rutiles from different geological environments. *Mineralogy and Petrology*, 45, 1–9.
- Herrero-Fernandez, M.P., Gonzalez-Calbet, J.M., Alario-Franco, M.A., Pernet, M., and Joubert, J.C. (1984) High pressure synthesis of mixed titanium-chromium oxyhydroxides. *Materials Research Bulletin*, 19, 1207–1213.
- Hong, S.H. and Åsbrink, S. (1982) The structure of the high-temperature modification of  $\text{V}_3\text{O}_5$  at 458 K. *Acta Crystallographica*, B38, 713–719.
- Hunter, W.C. and Smith, D. (1981) Garnet peridotite from Colorado Plateau ultramafic diatremes: Hydrates, carbonates, and comparative geothermometry. *Contributions to Mineralogy and Petrology*, 76, 312–320.
- Jones, A.P. (1989) Upper-mantle enrichment by kimberlitic or carbonatitic magmatism. In: K. Bell, ed., *Carbonates: Genesis and Evolution*, p. 448–463. Unwin Hyman Ltd, London.
- Libowitzky, E. (1999) Correlation of O-H stretching frequencies and O-H...O hydrogen bond lengths in minerals. *Monatshefte für Chemie*, 130, 1047–1059.
- Mandarino, J.A. (1981) The Gladstone-Dale relationship: Part IV. The compatibility concept and its application. *Canadian Mineralogist*, 19, 441–450.
- McDonough, W.F. and Sun, S.S. (1995) The composition of the Earth. *Chemical Geology*, 120, 223–253.
- McGetchin, T.R. and Silver, L.T. (1970) Compositional relations in minerals from kimberlite and related rocks in the Moses Rock dike, San Juan County, Utah. *American Mineralogist*, 55, 1738–1771.
- McGetchin, T.R., Silver, L.T., and Chodos, A.A. (1970) Titanoclinohumite: A possible mineralogical site for water in the upper mantle. *Journal of Geophysical Research*, 75, 255–259.
- Medenbach, O. and Schmetzer, K. (1978) Schreyerite,  $\text{V}_2\text{Ti}_3\text{O}_9$ , a new mineral. *American Mineralogist*, 63, 1182–1186.
- Messiga, B., Kienast, J.R., Rebay, G., Riccardi, M.P., and Tribuzio, R. (1999) Cr-rich magnesiochloritoid eclogites from the Monviso ophiolites (Western Alps, Italy). *Journal of Metamorphic Geology*, 17, 287–299.
- Moore, P.B. (1970) Edge-sharing silicate tetrahedra in the crystal structure of leucophoenicite. *American Mineralogist*, 55, 1146–1166.
- Papike, J.J. and Cameron, M. (1976) Crystal chemistry of silicate minerals of geophysical interest. *Reviews of Geophysics and Space Physics*, 1, 37–80.
- Ryerson, F.J. and Watson, E.B. (1987) Rutile saturation in magmas: Implications for Ti-Nb-Ta depletion in island arc basalts. *Earth and Planetary Science Letters*, 86, 225–239.
- Smith, D. (1987) Genesis of carbonate in pyrope from ultramafic diatremes on the Colorado Plateau, southwestern United States. *Contributions to Mineralogy and Petrology*, 97, 389–396.
- Wang, L., Essene, E.J., and Zhang, Y. (1999) Mineral inclusions in pyrope crystals from Garnet Ridge, Arizona, USA: Implications for processes in the upper mantle. *Contributions to Mineralogy and Petrology*, 135, 164–178.

MANUSCRIPT RECEIVED FEBRUARY 23, 1999  
 MANUSCRIPT ACCEPTED DECEMBER 25, 1999  
 PAPER HANDLED BY ROBERTA OBERTI